

Supplemental Data

Title:

Predicting Regional Respiratory Tissue and Systemic Concentrations of Orally Inhaled Drugs through a Novel PBPK Model

Authors:

Mayur K. Ladumor and Jashvant D. Unadkat

Affiliation:

Department of Pharmaceutics, School of Pharmacy, University of Washington, Seattle, WA (M.K.L., J.D.U.)

Journal Title:

Drug Metabolism and Disposition

Manuscript Number:

DMD-AR-2021-000789

Supplemental Method

Drug Deposition Model. The regional dose exposure for each respiratory tract region was calculated by multiplying the regional deposition efficiency (DE, dimensionless; sometimes referred to as deposition fraction, DF) with the overall OI dose (Eq. 1)

$$\text{Dose}_{\text{region}} = \text{DE}_{\text{region}} \times \text{OI dose} \quad (1)$$

During both the inhalation (inh) and exhalation (exh) cycles, each region acts as a filter (N=7 for the OI route) of the drug particles/droplets that flow through the region. The total and regional DE in the extrathoracic (ET2, oral passage), bronchial (BB), bronchiolar (bb), and alveolar (AL) regions were calculated by adding the DE in each filter during inh and exh cycle (Eqs. 2-7).

$$\text{DE}_{\text{ET2}} = \text{DE}_{1,\text{inh}} + \text{DE}_{7,\text{exh}} \quad (2)$$

$$\text{DE}_{\text{BB}} = \text{DE}_{2,\text{inh}} + \text{DE}_{6,\text{exh}} \quad (3)$$

$$\text{DE}_{\text{bb}} = \text{DE}_{3,\text{inh}} + \text{DE}_{5,\text{exh}} \quad (4)$$

$$\text{DE}_{\text{AL}} = \text{DE}_{4,\text{inh and exh}} \quad (5)$$

$$\text{DE}_{\text{total}} = \text{DE}_{\text{ET2}} + \text{DE}_{\text{BB}} + \text{DE}_{\text{bb}} + \text{DE}_{\text{AL}} \quad (6)$$

$$f_{\text{exhaled}} = 1 - \text{DE}_{\text{total}} \quad (7)$$

where f_{exhaled} is fraction exhaled.

The DE of each filter was calculated using the ICRP 66 deposition model (Eq. 8) as follows.

$$\text{DE}_j = \text{DE}_{j-1} \cdot \eta_j \cdot \xi_j \cdot \left(\frac{1}{\eta_{j-1}} - 1 \right), \text{ for } j = 1 \text{ to } 7 \quad (8)$$

where, j denotes the number of filters connected in series. η_j is the total filtration efficiency (dimensionless) of the j^{th} filter, i.e. the fraction of drug particles that enter and are deposited in the filter. ξ_j is a dimensionless factor that accounts for the different air volumes that pass through the filter.

The η_j for each filter was calculated using Eq. 9 as described below.

$$\eta_j = (\eta_{\text{ae},j}^2 + \eta_{\text{th},j}^2)^{1/2} \quad (9)$$

where, $\eta_{\text{ae},j}$ and $\eta_{\text{th},j}$ denote the aerodynamic (accounting for impaction and gravitational settling) and thermodynamic (accounting for particle diffusion by Brownian motion) filtration efficiencies (dimensionless), respectively and calculated as indicated in Tables S1 and S2.

ξ_j for each filter was calculated using Eq. 10 as described below.

$$\xi_j = \frac{\phi_j}{\phi_{j-1}} \quad (10)$$

where ϕ_j is the volumetric fraction (dimensionless) calculated by the cumulative volume of the preceding filters as indicated in Table S3.

To determine DE for the first filter (DE_1), prefiltration efficiency (η_0) at an imaginary prefilter (this filter reflects the potential loss of particles/droplets before entering the mouth) was calculated using Eq. 11.

$$\eta_0 = (1 - \eta_I) \quad (11)$$

where η_I is defined as inhalability (Eq. 12), defined as the fraction of drug particles in ambient air that enter the mouth before inhalation.

$$\eta_I = 1 - 0.5 (1 - [7.6 \times 10^{-4} d_{ae}^{2.8} + 1]^{-1}) + 1.0 \times 10^{-5} U^{2.75} \exp(0.055 \cdot d_{ae}) \quad (12)$$

where d_{ae} stands for aerodynamic diameter (μm), which is defined as the “diameter of unit density (1 g/mL) sphere that has same terminal settling velocity in air as the particle of interest”, and U denotes windspeed (m/s), which is defined as the rate at which air enters the respiratory tract via the mouth passage.

In order to calculate η_{th} , thermodynamic diameter (d_{th} (μm)) is defined as “diameter of a spherical particle that has the same diffusion coefficient (D ; Eq. 15) in air as the particle of interest”) was determined using Eq. 13.

$$d_{th} = d_{ae} \cdot \sqrt{\frac{\chi \cdot \rho_0}{\rho} \cdot \frac{C(d_{ae})}{C(d_{th})}} \quad (13)$$

where, ρ_0 and ρ are the unit density (1 g/mL) and drug density (g/mL), respectively; χ is the particle shape factor (dimensionless); $C(d_{ae})$ or $C(d_{th})$ is dimensionless slip correction factor for d_{ae} and d_{th} (Eq. 12), which is defined as “particle slip caused by the relative velocity of gas molecules at the particle surface”.

$$C(d) = 1 + \frac{\lambda}{d} \cdot \left[2.514 + 0.800 \exp\left(-0.55 \cdot \frac{d}{\lambda}\right) \right] \quad (14)$$

where, λ (μm) is a mean free path of the air molecules at 37°C, 100% relative humidity and 76 cm Hg atmospheric pressure. d is a diameter (d_{ae} or d_{th}). Convergence of Eq. 13 and 14 was achieved by using the initial setting such as $d_{th} = d_{ae} \cdot \sqrt{\chi/\rho}$.

$$D = \frac{k_B \cdot T \cdot C(d_{th})}{3 \cdot \pi \cdot \mu_{air} \cdot d_{th}} \quad (15)$$

where, k_B is the Boltzmann constant, T is the absolute body temperature in Kelvin and μ_{air} is the viscosity of air.

The hygroscopic growth of aerosol was integrated using Eq. 16 and 17, and the resulting new values of $d_{\text{ae},j}$ and D_j in each regional filter j were substituted for the d_{ae} and D in Tables S1 and S2.

$$d_{\text{ae},j} = d_{\text{ae},\infty} - (d_{\text{ae},\infty} - d_{\text{ae},0}) \cdot \left(\exp \left[\frac{-(10 \cdot t_{r,j})^{0.55}}{d_{\text{ae},0}} \right] \right)^{0.6} \quad (16)$$

$$D_j = D_0 - \left(\frac{d_{\text{ae},j} - d_{\text{ae},0}}{d_{\text{ae},\infty} - d_{\text{ae},0}} \right) \cdot (D_0 - D_{\infty}) \quad (17)$$

where $t_{r,j}$ is the residence time in regional filter j (Eqs. 20-23); $d_{\text{ae},0}$ and D_0 are the initial values of d_{ae} and D ; $d_{\text{ae},\infty}$ and D_{∞} are the equilibrium values of d_{ae} and D , respectively, as determined by hygroscopic growth factor (f_{hyg} , this is generally between 2-4-fold at equilibrium) using Eq. 16 and 17.

$$d_{\text{ae},\infty} = d_{\text{ae},0} \cdot f_{\text{hyg}} \quad (18)$$

$$D_{\infty} = D_0 / f_{\text{hyg}} \quad (19)$$

Residence time in second (s) for ET2, BB, bb and AL was calculated using Eqs. 20-23 considering the regional (n) dead space volume ($V_{D,n}$), tidal or inhalation volume (V), volumetric or inhalation flow rate (Q) and functional residual capacity (FRC).

$$t_{r,\text{ET2}} = 0.1 \quad (20)$$

$$t_{r,\text{BB}} = \frac{V_{D,\text{BB}}}{Q} \cdot \left(1 + \frac{0.5 \cdot V}{\text{FRC}} \right) \quad (21)$$

$$t_{r,\text{bb}} = \frac{V_{D,\text{bb}}}{Q} \cdot \left(1 + \frac{0.5 \cdot V}{\text{FRC}} \right) \quad (22)$$

$$t_{r,\text{AL}} = \frac{V - V_{D,\text{ET}} - [V_{D,\text{BB}} + V_{D,\text{bb}}] \cdot \left(1 + \frac{V}{\text{FRC}} \right)}{Q} \quad (23)$$

Drug Absorption Model. The mass balance equations for the regional respiratory absorption, lymphatic and systemic model are shown below.

ELF or Airway Liquid Compartment. The mass balance in the ELF compartment can be described using the following differential equation Eq. 24 and 25.

$$\frac{dA_{\text{ud},n}}{dt} = k_{t,n+1} \cdot A_{\text{ud},n+1} - k_{t,n} \cdot A_{\text{un},n} - K_{\text{dis},n} \cdot A_{\text{ud},n} \cdot (C_{s,n} - C_{\text{u},\text{dis},n}) \quad (24)$$

$$\begin{aligned} \frac{dC_{dis,n}}{dt} = \frac{1}{V_{F,n}} \cdot [& k_{t,n+1} \cdot A_{dis,n+1} \cdot V_{F,n} - k_{t,n} \cdot A_{dis,n} \cdot V_{F,n} + K_{dis,n} \cdot A_{ud,n} \cdot (C_{s,n} - C_{u_{dis,n}}) - \\ & k_{deg,n} \cdot C_{u_{dis,n}} \cdot V_{F,n} - PS_n \cdot (C_{u_{dis,n}} \cdot fui_{F,n} - C_{u_{E,n}} \cdot fui_{E,n}) - CL_{inf,F-E} \cdot C_{u_{dis,n}} + \\ & CL_{eff,E-F} \cdot C_{u_{E,n}}] \end{aligned} \quad (25)$$

where $A_{ud,n}$ is the undissolved drug amount in the n^{th} ELF compartment of the respiratory tract; $k_{t,n}$ represent the transit rate constants in the n^{th} compartment; $K_{dis,n}$ represents the dissolution rate constant of the undissolved drug amount in the n^{th} compartment (Eq. 26); $C_{s,n}$ is drug solubility in the n^{th} compartment; $V_{F,n}$ represent the ELF volume of the n^{th} compartment; $C_{u_{dis,n}}$ denotes the unbound dissolved drug concentration in the n^{th} ELF compartment; subscript F, E and n denote ELF compartment, epithelial compartment and region of the respiratory compartment, respectively; $k_{deg,n}$ is the first-order degradation rate constant in the n^{th} ELF compartment; fui denote fraction of unionized drug; PS, permeability-surface area product; $CL_{inf,F-E}$, active influx transporter-mediated drug clearance from ELF to epithelial direction; $CL_{eff,E-F}$, active efflux transporter-mediated drug clearance from epithelial to ELF direction.

Dissolution rate constant. $K_{dis,n}$ or z-factor was determined by Hintz - Johnson model (Hintz and Johnson, 1989) as shown in Eq. 26.

$$K_{dis,n} = \frac{3 \cdot D}{\rho \cdot r \cdot h} \quad (26)$$

where r is the particle radius ($r = d_e/2$; d_e is equivalent volume diameter and was calculated from d_{ae} (Eq. 27)); h is the diffusion layer thickness ($h = r$ if $r < 30 \mu m$, otherwise $h = 30 \mu m$); D was calculated using Eq. 15 considering the viscosity of simulated lung lining fluid.

$$d_e = d_{ae} \cdot \sqrt{\frac{\chi \cdot \rho_0}{\rho} \cdot \frac{C(d_{ae})}{C(d_e)}} \quad (27)$$

where d_e was converged as described in Eq. 13 and 14 and $C(d_e)$ was calculated according to Eq. 14.

Fraction of unionized drug. fui values for the ELF, epithelial, subepithelial, and blood compartments of the regional respiratory tract were determined by the Henderson-Hasselbalch equation (Po and Senozan, 2001) using pH value of the regional compartment and drug acid dissociation constant (pK_a) data (Eqs. 28-33).

$$fui = 1 \text{ for neutral drug} \quad (28)$$

$$fui = 1 / [1 + (10^{pH-pK_a})] \text{ for monoprotic acid drug} \quad (29)$$

$$fui = 1 / [1 + (10^{pH-pK_{a1}} + 10^{2 \cdot pH - pK_{a1} - pK_{a2}})] \text{ for diprotic acid } (pK_{a1} < pK_{a2}) \quad (30)$$

$$f_{ui} = 1 / [1 + (10^{pK_a - pH})] \text{ for monoprotic base drug} \quad (31)$$

$$f_{ui} = 1 / [1 + (10^{pK_{a2} - pH} + 10^{pK_{a1} + pK_{a2} - 2 \cdot pH})] \text{ for diprotic base } (pK_{a1} < pK_{a2}) \quad (32)$$

$$f_{ui} = 1 / [1 + (10^{pK_{a,base} - pH} + 10^{pH - pK_{a,acid}})] \text{ for zwitterion drug} \quad (33)$$

Fraction of unbound drug. If experimental f_u values are not available, f_u for the epithelial and subepithelial compartments of the regional respiratory tract was calculated using the fraction unbound in plasma ($f_{u,plasma}$), the tissue to plasma partition coefficient ($K_{p,tissue-pls}$; Eq. 35) and the interstitial to plasma partition coefficient ($K_{p,int-pls}$; Eqs. 36 and 38) (Schmitt et al., 2008). Lung includes the BB, bb and AL regions. The tissue composition of the ET2 region was assumed to be the same as lung, so the K_p of the ET2 region was identical to the lung tissue.

$$f_{u,F,n} = 1 \quad (34)$$

$$f_{u,E,n} = f_{u,plasma} / K_{p,tissue-pls} \quad (35)$$

$$f_{u,S,n} = f_{u,plasma} / K_{p,int-pls} \quad (36)$$

$$f_{u,B,n} = f_{u,plasma} / BP \quad (37)$$

$$K_{p,int-pls} = (f_{water,int} + \text{protein ratio} \cdot (1/(f_{u,plasma} - f_{water,plasma}))) \cdot f_{u,plasma} \quad (38)$$

Membrane permeability. Apical epithelial membrane permeability or the permeability surface area product (PS) between ELF and epithelial compartment was calculated for each region using the apparent permeability ($P_{app, calu-3}$) obtained from the *in vitro* bronchial epithelial calu-3 model and the surface area (SA) of each respiratory tract region (Eq. 39). To calculate regional P_{app} (Eq. 40), $P_{app, calu-3}$ was then corrected by regional membrane thickness scalar (RT) through thickness, h_{mem} , of the epithelial compartments of BB region and other regions of the respiratory tract (Eq. 41). For the purpose of making the model more general, we used the linear regression model (Eq. 42, $R^2 = 0.93$) for $P_{app, calu-3}$ developed by Brillault and colleagues (Brillault et al., 2010). This model (Eq. 42) is based on *in vitro* $P_{app, calu-3}$ of fluoroquinolones compounds in the presence of a P-glycoprotein (P-gp) inhibitor such as valspodar (PSC-833) and the partition coefficients between octanol and a pH 7.4 buffered solution (logD).

$$PS_n = P_{app,n} \cdot SA_n \quad (39)$$

$$P_{app,n} = RT_n \cdot P_{app,calu-3} \quad (40)$$

$$RT_n = \frac{h_{mem, BB}}{h_{mem, n}} \quad (41)$$

$$P_{app,calu-3} (10^{-6} \text{ cm/s}) = 6.1 \cdot \log D + 7.5 \quad (42)$$

Epithelial or Intracellular Compartment. The mass balance in the epithelial compartment can be described using the following differential Eq. 43.

$$\begin{aligned} \frac{dC_{E,n}}{dt} = \frac{1}{V_{E,n}} \cdot [& PS_n \cdot (Cu_{dis,n} \cdot fui_{F,n} - Cu_{E,n} \cdot fui_{E,n}) + CL_{inf,F-E} \cdot Cu_{dis,n} - CL_{eff,E-F} \cdot Cu_{E,n} - PS_n \cdot \\ & (Cu_{E,n} \cdot fui_{E,n} - Cu_{S,n} \cdot fui_{S,n}) + CL_{inf,S-E} \cdot Cu_{S,n} - CL_{eff,E-S} \cdot Cu_{E,n} - CL_{int,met,n} \cdot \\ & Cu_{E,n} - (k_{on,n} \cdot Cu_{E,n} \cdot FA - k_{off,n} \cdot C_{conj,E,n}) \cdot V_{E,n}] \end{aligned} \quad (43)$$

where V, Cu, and Q_B denote the volume, unbound drug concentration and blood flow of the tissue, respectively. PS and fui are permeability surface area product and fraction of unionized drug, respectively. CL_{int,met} is intrinsic clearance of drug mediated by metabolism. k_{on} and k_{off} are the second order association and first order dissociation rate constants for tissue retention, respectively. Subscript E, S and n denote epithelial compartment, subepithelial compartment and region of the respiratory compartment, respectively. CL_{inf,F-E}, active influx transporter-mediated drug clearance from ELF to epithelial direction; CL_{eff,E-F}, active efflux transporter-mediated drug clearance from epithelial to ELF direction; CL_{inf,S-E}, active influx transporter-mediated drug clearance from subepithelial to epithelial direction; CL_{eff,E-S}, active efflux transporter-mediated drug clearance from epithelial to subepithelial direction; FA, fatty acid concentration.

Subepithelial or Interstitial Compartment. The mass balance in subepithelial compartment can be described using the following differential Eq. 44.

$$\begin{aligned} \frac{dC_{S,n}}{dt} = \frac{1}{V_{S,n}} \cdot [& PS_n \cdot (Cu_{E,n} \cdot fui_{E,n} - Cu_{S,n} \cdot fui_{S,n}) - PS_n \cdot (Cu_{S,n} \cdot fui_{S,n} - Cu_{B,n} \cdot fui_{B,n}) - \\ & CL_{inf,E-S} \cdot Cu_{S,n} + CL_{eff,S-E} \cdot Cu_{E,n} + Q_{L,n} \cdot Cu_{S,n}] \end{aligned} \quad (44)$$

where V, Cu, Q_B and Q_L denote the volume, unbound drug concentration, blood flow and lymph flow of the tissue, respectively. PS and fui are permeability surface area product and fraction of unionized drug, respectively. Subscript E, S and n denote epithelial compartment, subepithelial compartment and region of the respiratory compartment, respectively; CL_{inf,E-S}, active influx transporter-mediated drug clearance from epithelial to subepithelial direction; CL_{eff,S-E}, active efflux transporter-mediated drug clearance from subepithelial to epithelial direction.

Blood or Vascular Compartment. The mass balance in the blood compartment of ET2, BB and bb regions can be described using the following differential Eq. 45.

$$\frac{dC_{B,n}}{dt} = \frac{1}{V_{B,n}} \cdot [PS_n \cdot (Cu_{S,n} \cdot fui_{S,n} - Cu_{B,n} \cdot fui_{B,n}) + Q_{B,n} \cdot C_{ab,n} - (Q_{B,n} - Q_{L,n}) \cdot C_{B,n}] \quad (45)$$

The mass balance in the blood compartment of AL region can be described using the following differential Eq. 46.

$$\frac{dC_{B,AL}}{dt} = \frac{1}{V_{B,AL}} \cdot [PS_{AL} \cdot (C_{u,S,AL} \cdot f_{ui,S,AL} - C_{u,B,AL} \cdot f_{ui,B,AL}) + Q_{B,AL} \cdot C_{vb} - (Q_{B,AL} - Q_{L,AL}) \cdot C_{B,AL}] \quad (46)$$

where V , C_u , Q_B and Q_L denote the volume, unbound drug concentration, blood flow and lymph flow of the tissue, respectively. PS and f_{ui} are permeability surface area product and fraction of unionized drug, respectively. Subscript S and B denote subepithelial compartment and blood compartment, respectively.

Lymph node compartment (LN). The mass balance in the lymph node compartment of AL region can be described using the following differential Eq. 47.

$$\frac{dC_{LN}}{dt} = \frac{1}{V_{LN}} \cdot [Q_{L,ET2} \cdot C_{S,ET2} + Q_{L,BB} \cdot C_{S,BB} + Q_{L,bb} \cdot C_{S,bb} + Q_{L,AL} \cdot C_{S,AL} - Q_{L,LN} \cdot C_{LN}] \quad (47)$$

where V , C and Q_L denote the volume, concentration and lymph flow of the tissue, respectively. LN , $ET2$, BB , bb , AL , S and B denote the lymph node, extrathoracic (oral passage), bronchial, bronchiolar, alveolar, subepithelial and blood, respectively.

Whole-body PBPK model. The mass balance equations for the whole-body PBPK model are shown below (Eqs. 48-54).

Arterial blood compartment (ab).

$$\begin{aligned} \frac{dC_{ab}}{dt} = \frac{1}{V_{ab}} \cdot [& (Q_{B,AL} - Q_{L,AL}) \cdot C_{B,AL} - Q_{B,ET2} \cdot C_{ab} - Q_{B,BB} \cdot C_{ab} - Q_{B,bb} \cdot C_{ab} - Q_{B,adipose} \cdot C_{ab} - \\ & Q_{B,bone} \cdot C_{ab} - Q_{B,brain} \cdot C_{ab} - Q_{B,heart} \cdot C_{ab} - Q_{B,kidney} \cdot C_{ab} - Q_{B,muscle} \cdot C_{ab} - \\ & Q_{B,skin} \cdot C_{ab} - (Q_{B,liver} - Q_{B,gut} - Q_{B,spleen} - Q_{B,pancreas}) \cdot C_{ab} - Q_{B,gut} \cdot C_{ab} - \\ & Q_{B,spleen} \cdot C_{ab} - Q_{B,pancreas} \cdot C_{ab}] \end{aligned} \quad (48)$$

where V , C , Q_B and Q_L denote the volume, concentration, blood flow and lymph flow of the tissue, respectively. ab , $ET2$, BB , bb , and AL denote the arterial blood, extrathoracic (oral passage), bronchial, bronchiolar, and alveolar, respectively.

Venous blood compartment (vb).

$$\begin{aligned} \frac{dC_{vb}}{dt} = \frac{1}{V_{vb}} \cdot [& (Q_{B,ET} - Q_{L,ET}) \cdot C_{B,ET} + (Q_{BB} - Q_{L,BB}) \cdot C_{B,BB} + (Q_{bb} - Q_{L,bb}) \cdot C_{B,bb} - Q_{B,AL} \cdot \\ & C_{vb} + Q_{L,LN} \cdot C_{LN} + Q_{B,adipose} \cdot \frac{C_{adipose}}{K_{p_{adipose}/BP}} + Q_{B,bone} \cdot \frac{C_{bone}}{K_{p_{bone}/BP}} + Q_{B,brain} \cdot \\ & \frac{C_{brain}}{K_{p_{brain}/BP}} + Q_{B,heart} \cdot \frac{C_{heart}}{K_{p_{heart}/BP}} + Q_{B,kidney} \cdot \frac{C_{kidney}}{K_{p_{kidney}/BP}} + Q_{B,muscle} \cdot \\ & \frac{C_{muscle}}{K_{p_{muscle}/BP}} + Q_{B,skin} \cdot \frac{C_{skin}}{K_{p_{skin}/BP}} + Q_{B,liver} \cdot \frac{C_{liver}}{K_{p_{liver}/BP}} - CL_{renal} \cdot f_{uB} \cdot C_{vb} + \\ & Q_{B,forearm} \cdot C_{forearm}] \end{aligned} \quad (49)$$

where V , C , Q_B and Q_L denote the volume, concentration, blood flow and lymph flow of the tissue, respectively. C_{vb} denotes the venous blood concentration, K_p denotes the tissue-to-plasma partition coefficient of the tissue, and f_{uB} denotes the fraction unbound in blood. ET2, BB, bb, and AL denote the extrathoracic (oral passage), bronchial, bronchiolar, and alveolar, respectively.

Non-eliminating tissue.

$$\frac{dC_{\text{tissue}}}{dt} = \frac{1}{V_{\text{tissue}}} \cdot \left[Q_{B,\text{tissue}} \cdot \left(C_{ab} - \frac{C_{\text{tissue}}}{K_{p\text{tissue}}/BP} \right) \right] \quad (50)$$

where V_{tissue} , C_{tissue} , and $Q_{B,\text{tissue}}$ denote the volume, concentration, and blood flow of the tissue, respectively. C_{ab} , $K_{p\text{tissue}}$, and BP denote the arterial blood concentration, tissue-to-plasma partition coefficient, and blood-to-plasma concentration ratio, respectively.

Eliminating tissue (liver).

$$\begin{aligned} \frac{dC_{\text{liver},B}}{dt} = \frac{1}{V_{\text{liver}}} \cdot \left[(Q_{B,\text{liver}} - Q_{B,\text{gut}} - Q_{B,\text{spleen}} - Q_{B,\text{pancreas}}) \cdot C_{ab} + Q_{B,\text{gut}} \cdot \frac{C_{\text{gut}}}{K_{p\text{gut}}/BP} + Q_{\text{spleen}} \cdot \right. \\ \left. \frac{C_{\text{spleen}}}{K_{p\text{spleen}}/BP} + Q_{B,\text{pancreas}} \cdot \frac{C_{\text{pancreas}}}{K_{p\text{pancreas}}/BP} - Q_{B,\text{liver}} \cdot C_{\text{liver},B} - PS_{B-IS \text{ or } IS-B} \cdot \right. \\ \left. (Cu_{\text{liver},B} \cdot fui_{\text{liver},B} - Cu_{\text{liver},IS} \cdot fui_{\text{liver},IS}) \right] \quad (51) \end{aligned}$$

$$\begin{aligned} \frac{dC_{\text{liver},IS}}{dt} = \frac{1}{V_{\text{liver},IS}} \cdot \left[PS_{B-IS \text{ or } IS-B} \cdot (Cu_{\text{liver},B} \cdot fui_{\text{liver},B} - Cu_{\text{liver},IS} \cdot fui_{\text{liver},IS}) + PS_{IS-IC \text{ or } IC-IS} \cdot \right. \\ \left. (Cu_{\text{liver},IC} \cdot fui_{\text{liver},IC} - Cu_{\text{liver},IS} \cdot fui_{\text{liver},IS}) - CL_{\text{inf},IS-IC} \cdot Cu_{\text{liver},IS} + \right. \\ \left. CL_{\text{eff},IC-IS} \cdot Cu_{\text{liver},IC} \right] \quad (52) \end{aligned}$$

$$\begin{aligned} \frac{dC_{\text{liver},IC}}{dt} = \frac{1}{V_{\text{liver},IC}} \cdot \left[PS_{IS-IC \text{ or } IC-IS} \cdot (Cu_{\text{liver},IS} \cdot fui_{\text{liver},IS} - Cu_{\text{liver},IC} \cdot fui_{\text{liver},IC}) + CL_{\text{inf},IS-IC} \cdot \right. \\ \left. Cu_{\text{liver},IS} - CL_{\text{eff},IC-IS} \cdot Cu_{\text{liver},IC} - CL_{\text{int},H} \cdot Cu_{\text{liver},IC} \right] \quad (53) \end{aligned}$$

Subscript B, IS and IC denote blood, interstitial and intracellular compartments, respectively. where V , C_u and Q_B denote the volume, unbound drug concentration and blood flow of the tissue, respectively. PS and f_{ui} are permeability surface area product and fraction of unionized drug, respectively. CL_{inf} and CL_{eff} are active influx and efflux transporter-mediated drug clearance, respectively. C_{ab} , $K_{p\text{tissue}}$, and BP denote the arterial blood concentration, tissue-to-plasma partition coefficient, and blood-to-plasma concentration ratio, respectively. $CL_{\text{int},H}$, denotes the intrinsic hepatic drug metabolic clearance.

Forearm (peripheral sampling) compartment.

$$\frac{dC_{\text{forearm}}}{dt} = \frac{1}{V_{\text{forearm}}} \cdot \left[Q_{B,\text{anastomoses}} \cdot C_{ab} + Q_{B,\text{forearm muscle}} \cdot \frac{C_{\text{forearm muscle}}}{K_{p\text{muscle}/BP}} + Q_{B,\text{forearm skin}} \cdot \frac{C_{\text{forearm skin}}}{K_{p\text{skin}/BP}} + Q_{B,\text{forearm adipose}} \cdot \frac{C_{\text{forearm adipose}}}{K_{p\text{adipose}/BP}} - Q_{B,\text{forearm}} \cdot C_{\text{forearm}} \right] \quad (54)$$

where V , C , and Q_B denote the volume, concentration, and blood flow of the tissue, respectively. C_{ab} , $K_{p\text{tissue}}$, and BP denote the arterial blood concentration, tissue-to-plasma partition coefficient, and blood-to-plasma concentration ratio, respectively.

In vitro to in vivo extrapolation (IVIVE). Drug metabolizing enzyme or transporter (DMET) mediated *in vivo* intrinsic clearance in reference organ such as the liver ($CL_{\text{int,ref organ}}$; in L/h unit) can be determined by *in vitro* intrinsic clearance ($CL_{\text{int,in vitro}}$; in $\mu\text{L}/\text{min}/\text{mg}$ subcellular fraction protein or $\mu\text{L}/\text{min}/\text{number of cells}$) or by the *vitro* unbound Michaelis-Menten kinetics for the enzyme (maximum enzymatic reaction rate (V_{max})/ substrate affinity (K_m)) or transporter (maximum transport rate (J_{max})/ K_m)) through IVIVE (Eqs. 55-58).

$$CL_{\text{int,ref organ}} = CL_{\text{int,in vitro}} \times \text{PSF} \times \text{organ weight} \times 60 \times 10^{-6} \quad (55)$$

$$CL_{\text{int,RT}} = CL_{\text{int,ref organ}} \times RA_{\text{RT}} \quad (56)$$

$$RA_{\text{RT}} = \frac{A_{\text{protein,RT}}}{A_{\text{protein,ref organ}}} \quad (57)$$

$$A_{\text{protein,organ}} = A_{\text{protein,subcellular fraction}} \times \text{PSF} \times \text{Organ weight} \times 10^{-6} \quad (58)$$

where PSF is the physiological scaling factor (yield of the subcellular fraction from whole organ (in mg subcellular fraction protein/g organ or number of cells/g of organ)); organ weight is the subject's organ weight (in g); ref organ, RT and RA denote the reference organ (e.g. liver), respiratory tract regions (ET2, BB, bb and AL) and relative protein abundance, respectively; $A_{\text{protein,organ}}$ is the protein abundance of DMET per whole organ (in μmol unit); $A_{\text{protein,subcellular}}$ is the protein abundance of DMET per subcellular fraction of organ (in pmol/mg subcellular fraction protein unit); 60×10^{-6} and 10^{-6} are unit conversion factors to convert the $CL_{\text{int,ref organ}}$ to L/h and $A_{\text{protein,organ}}$ to μmol , respectively.

Supplemental Tables

Table S1. Algebraic expressions for aerodynamic filtration efficiency in the ICRP 66 deposition model (ICRP, 1995).

Aerodynamic filtration efficiency ($\eta_{ae} = 1 - \exp(-aR^P)$)					
Phase	Filter (j)	Region	a	R	P
Inhalation	1	ET ₂ [§]	$1.1 \cdot 10^{-4}$	$d_{ae}^2 \cdot (Q \cdot SF_{BB}^3)^{0.6} \cdot (V \cdot SF_{BB}^2)^{-0.2}$	1.4
	2	BB	$4.08 \cdot 10^{-6}$	$d_{ae}^2 \cdot Q \cdot SF_{BB}^{2.3}$	1.152
	3	bb	0.1147	$(0.056 + t_{r,bb}^{1.5}) \cdot d_{ae}^{tr,bb \wedge -0.25}$	1.173
	4	AL	$0.146 \cdot SF_{AL}^{0.98}$	$d_{ae}^2 \cdot t_{r,AL}$	0.6495
Exhalation	5	bb	0.1147	$(0.056 + t_{r,bb}^{1.5}) \cdot d_{ae}^{tr,bb \wedge -0.25}$	1.173
	6	BB	$2.04 \cdot 10^{-6}$	$d_{ae}^2 \cdot Q \cdot SF_{BB}^{2.3}$	1.152
	7	ET ₂ [§]	$1.1 \cdot 10^{-4}$	$d_{ae}^2 \cdot (Q \cdot SF_{BB}^3)^{0.6} \cdot (V \cdot SF_{BB}^2)^{-0.2}$	1.4

a and P are constants and R is a parameter, which is drug- and system-dependent. a, P and R were obtained from ICRP 66 deposition model (ICRP, 1995). ET₂, extrathoracic (oral passage); BB, bronchial; bb, bronchiolar; AL, alveolar; SF_{BB}, scale factor for trachea; SF_{bb}, scale factor for bronchiolar; SF_{AL}, scale factor for alveolar; V, tidal or inhalation volume; Q, volumetric or inhalation flow rate; t_{r,bb}, residence time for bronchiolar; t_{r,AL}, residence time for alveolar; d_{ae}, aerodynamic particle diameter.

[§] Aerodynamic filtration efficiency for ET₂ region was calculated as $\eta_{ae} = 1 - 1/(-aR^P + 1)$

Table S2. Algebraic expressions for thermodynamic filtration efficiency in the ICRP 66 deposition model (ICRP, 1995).

Thermodynamic regional deposition efficiency ($\eta_{th} = 1 - \exp(-aR^P)$)					
Phase	Filter (j)	Region	a	R	P
Inhalation	1	ET ₂	9	$D \cdot (Q \cdot SF_{BB})^{-0.25}$	0.5
	2	BB	$22.02 \cdot SF_{BB}^{1.24} \cdot \psi_{th}$	$D \cdot t_{r,BB}$	0.6391
	3	bb	$-76.8 + 167 \cdot SF_{bb}^{0.65}$	$D \cdot t_{r,bb}$	0.5676
	4	AL	$170 + 103 \cdot SF_{AL}^{2.13}$	$D \cdot t_{r,AL}$	0.6101
Exhalation	5	bb	$-76.8 + 167 \cdot SF_{bb}^{0.65}$	$D \cdot t_{r,bb}$	0.5676
	6	BB	$22.02 \times SF_{BB}^{1.24} \cdot \psi_{th}$	$D \cdot t_{r,BB}$	0.6391
	7	ET ₂	9	$D \cdot (Q \cdot SF_{BB})^{-0.25}$	0.5

where a and P are constants and R is a parameter, which is drug- and system-dependent. a, P and R were obtained from ICRP 66 deposition model (ICRP, 1995). ET₂, extrathoracic (oral passage); BB, bronchial; bb, bronchiolar; AL, alveolar; SF_{BB}, scale factor for trachea; SF_{bb}, scale factor for bronchiolar; SF_{AL}, scale factor for alveolar; Q, volumetric or inhalation

flow rate; $t_{r,bb}$, residence time for bronchial; $t_{r,bb}$, residence time for bronchiolar; $t_{r,AL}$, residence time for alveolar; D , diffusion coefficient; d_{th} , thermodynamic particle diameter. # Ψ_{th} is an empirical correction factor to allow for enhancement of thermodynamic deposition caused by nonlaminar bronchial airflow and calculated $\Psi_{th} = 1 + 100 \exp[-[\log_{10}(100 + 10/(d_{th}^{0.9}))]^2]$

Table S3. Algebraic expressions for a volumetric fraction in the ICRP 66 deposition model (ICRP, 1995).

Phase	Filter (j)	Region	Volumetric fraction (ϕ_j)
Inhalation	1	ET ₂	1
	2	BB	$1 - (V_{D,ET2}/V)$
	3	bb	$1 - ((V_{D,ET2} + V_{D,BB,p})/V)$
	4	AL	$1 - ((V_{D,ET2} + V_{D,BB,p} + V_{D,bb,p})/V)$
Exhalation	5	bb	$1 - ((V_{D,ET2} + V_{D,BB,p})/V)$
	6	BB	$1 - (V_{D,ET2}/V)$
	7	ET ₂	1

FRC, functional residual capacity; V_D , dead space volume; ET₂, extrathoracic (oral passage); BB, bronchial; bb, bronchiolar; AL, alveolar; V , tidal or inhalation volume. $V_{D,BB,p}$ and $V_{D,bb,p}$ were calculated as $V_{D,BB,p} = V_{D,BB} \times (1 + (V/FRC))$ and $V_{D,bb,p} = V_{D,bb} \times (1 + (V/FRC))$, respectively.

Table S4. Respiratory tissue-specific input parameters for the OI-PBPK model (ICRP, 1995; Patton and Byron, 2007).

	Extra-thoracic (ET2)	Bronchial (BB)	Bronchiolar (bb)	Alveolar (AL)
Surface area (SA, cm ²)	450	290	2400	1475000
ELF thickness (um)	15	11	6	0.07
Epithelial thickness (cm)	50	55	15	0.361
Subepithelial thickness (cm)	15	500	20	1.86
ELF volume (mL)	0.68	0.32	1.44	10.33
Epithelial volume (mL)	2.25	1.60	3.60	276
Subepithelial volume (mL)	0.68	14.50	4.80	274
Blood volume (mL)	17.73	11.43	94.57	556.5
Tissue volume (mL)	2.93	16.1	8.4	550
Density (g/mL)	1	1	1	1
Blood flow rate (L/h)	1.63	1.05	8.70	390.00
Respiratory transit time (h)	0.24	2.4	12	1200
Respiratory transit rate (1/h)	4.17	0.417	0.083	0.00083
Lymph flow (L/h)	0.002	0.0001	0.009	0.42
pH of ELF*	6.6	6.6	6.6	6.6
pH of epithelial*	6.69	6.69	6.69	6.69
pH of subepithelial#	7.35	7.35	7.35	7.35
pH of blood#	7.4	7.4	7.4	7.4

1. Volume of ELF, epithelial and subepithelial compartments of each region of the respiratory tract were calculated multiplying the SA of the compartment by the thickness of the compartment.

2. Volume of blood compartment of AL region was calculated by multiplying the total blood volume (5.3 L for adult male, ICRP Valentin) by the % total blood volume of pulmonary tissue (10.5% for adult male, ICRP Valentin).

3. Volume of blood compartment of BB and bb regions were calculated by multiplying the total blood volume (5.3 L for adult male, ICRP Valentin) by the % total blood volume of bronchial tissue (2% for adult male, ICRP Valentin) and $SA_{BB \text{ or } bb}/SA_{BB+bb}$.

4. Blood flow of BB and bb regions were calculated by multiplying cardiac output (390 L/h for adult male, ICRP Valentin) by the % cardiac output of bronchial tissue (2.5% for adult male, ICRP Valentin) and $SA_{BB \text{ or } bb}/SA_{BB+bb}$.

5. Blood flow or volume of ET2 region were calculated by multiplying blood flow or volume of BB region by the SA_{ET2}/SA_{BB} due to unavailability of data and SA of ET2 is comparable to that of BB region.

6. Lymph flow of each region was calculated by dividing plasma flow (multiplying blood flow of each region by 1- hematocrit (0.46)) by 500 (Shah et al., 2012).

*(Gaohua et al., 2015)

*(Burton, 2001)

Table S5. Summary of system-dependent parameters for the reference adult male (Valentin, 2002)*

	Organ Volume (L)	Blood flow (% of CO)	Blood flow (L/h)
Adipose	18.2	5	19.50
Bone	10.5	5	19.50
Brain	1.45	12	46.80
Gut**	1.21	15	58.50
Heart	0.33	4	15.60
Kidney	0.31	19	74.10
Liver	1.8	25.5	99.45
Hepatic artery		6.5	25.35
Muscle	29	17	68.25
Skin	3.3	5	19.50
Spleen	0.15	3	11.70
Pancreas	0.14	1	3.90
Lymph nodes	0.274\$	1.7	6.63
Blood	5.3		

*Reference values for adult male: 35 years of age, 73 kg of body weight, 176 cm of height and 390 L/h of cardiac output (CO). ** Gut combines oesophagus, stomach, small and large intestine volumes and flows; gut contents were not included in the gut volume.

\$(Shah et al., 2012)

Table S6. Summary of input parameters for the morphine OI-PBPK model.

Parameter	Value/method/model	Reference
Physicochemical and blood binding		
MW (g/mol)	285.34	(Emoto et al., 2017)
Log $P_{o:w}$	0.77	(Emoto et al., 2017)
pKa1, pKa2	9.63, 7.93	(Emoto et al., 2017)
Compound type	Ampholyte	
B/P	1.08	(Emoto et al., 2017)
fu	0.62	(Emoto et al., 2017)
Distribution		
Model	Full PBPK	(Emoto et al., 2017)
Method	Rodgers et al Method 2	(Emoto et al., 2017)
Organ/tissue Kp		(Emoto et al., 2017)
Adipose	1.079	
Bone	2.092	
Brain	1.517	
Gut	7.228	
Heart	7.737	
Kidney	4.187	
Liver	12.417	
Lung	1.970	
Muscle	6.597	
Skin	3.521	
Spleen	7.273	
Pancreas	4.771	
Kp scalar	1	
Elimination		
CL _R in L/h	8	(Emoto et al., 2017)
Organ/tissue	Liver	(Emoto et al., 2017)
Pathway: 6MG		
Enzyme	UGT2B7	
V _{max} (pmol/min/mg protein)	1917	
K _m (μM)	115.8	
fu _{mic}	1	
V _{max} (μmol/h)	6625.15	
Pathway: 3MG		

Enzyme	UGT2B7	
V_{\max} (pmol/min/mg protein)	9250	
K_m (μ M)	115.8	
$f_{u_{mic}}$	1	
V_{\max} (μ mol/h)	31968	
Transport		
Organ/Tissue	Liver	(Emoto et al., 2017)
$CL_{PD, in vitro}$ (mL/min/ 10^6 cells)	0.003	
$CL_{PD, organ}$ (L/h)	32.1	
$f_{u_{IC}}$	0.05	Eq. 35
$f_{u_{IS}}$	1	Eq. 36
Organ/Tissue	Liver	
Transporter	SLC22A1 (OCT1)	
Location	Sinusoidal	
Function	Influx	
J_{\max} (pmol/min/ 10^6 cells)	29	
K_m (μ M)	3.4	
$f_{u_{inc}}$	1	
RAF/REF	5.1	
J_{\max} (μ mol/h)	1584.4	Eq. 55
Liver: PSF		
HPGL (hepatocellularity /g liver or 10^6 cells/g liver)	99	(Barter et al., 2007)
Liver weight (g)	1800	Table S5
Liver: UGT2B7		
A_{UGT2B7} (pmol/mg microsomal protein)	75.2	(Ladumor et al. 2019)
A_{UGT2B7} (μ mol/liver tissue)	4.3	Eq. 58
Liver: OCT1		
A_{OCT1} (pmol/mg membrane protein)	4.45	
A_{OCT1} (μ mol/liver tissue)	0.30	Eq. 58
Liver: PSF		
MMPGL (mg microsomal protein/g liver)	32	(Barter et al., 2007)
MMePGL (mg membrane protein/g liver)	37	(Prasad et al., 2014)
Lung: UGT2B7		
A_{UGT2B7} (pmol/mg microsomal protein) ¹	0.15	

A_{UGT2B7} ($\mu\text{mol/lung tissue}$)	BB: 9E-6 bb: 5E-6 AL: 3E-4	Eq. 58
Lung: OCT1		
A_{OCT1} (pmol/mg membrane protein) ²	0.22	(Wang et al. 2015)
A_{OCT1} ($\mu\text{mol/lung tissue}$)	BB: 1E-5 bb: 7E-6 AL: 5E-4	Eq. 58
Lung: PSF		
MMPGLu (mg microsomal protein/g lung)	3.8	(Pacifici et al., 1988)
MMePGLu (mg membrane protein/g lung) ³	3.8	(Pacifici et al., 1988)

MW, molecular weight; Log $P_{o:w}$, n-octanol/water partition coefficient; pK_a , acid dissociation constant; B/P, blood/plasma ratio; f_u , fraction of unbound drug in the plasma; HSA, human serum albumin; K_p , tissue to plasma partition coefficient; V_{max} , maximum enzymatic reaction rate; J_{max} , maximum transport rate; K_m , substrate affinity or Michaelis-Menten constant; $f_{u,mic}$, fraction of unbound drug in the *vitro* microsomal incubation; $f_{u,inc}$, fraction of unbound drug in the *vitro* incubation; $f_{u,IC}$, fraction of unbound drug in the intracellular compartment; $f_{u,IS}$, fraction of unbound drug in the interstitial compartment; $CL_{PD, in vitro}$, *in vitro* passive diffusion clearance; $CL_{PD, organ}$, *in vivo* whole organ passive diffusion clearance; CL_R , renal clearance; RAF/REF, relative activity factor/relative expression factor; PSF, physiological scaling factor (yield of the subcellular fraction from whole organ (in mg subcellular fraction protein/g organ)); A_{DMET} is the protein abundance of drug metabolizing enzymes and transporters (DMET); UGT, uridine 5'-diphospho-glucuronosyltransferase; OCT, organic cation transporter; MMPGL, mg microsomal protein per gram of human liver; MMePGL, mg total membrane protein per gram of human liver; MMPGLu, mg microsomal protein per gram of human lung; MMePGLu, mg total membrane protein per gram of human lung; HPGL, hepatocellularity per gram of human liver.

1. UGT2B7 protein abundance per subcellular fraction was calculated by multiplying the liver subcellular protein abundance by the ratio of lung (BB, bb, and AL) to liver tissue mRNA expression (Somers et al., 2007).
2. OCT1 protein abundance per subcellular fraction was calculated by multiplying the liver subcellular protein abundance by the ratio of lung (BB, bb, and AL) to liver tissue transporter plasma membrane expression (Ohtsuki et al., 2012; Sakamoto et al., 2013).
3. MMePGLu was assumed similar to the MMPGLu.

Table S7. Summary of input parameters for the nicotine OI-PBPK model.

Parameter	Value/method/model	Reference
Physicochemical and blood binding		
MW (g/mol)	162.2	(Kovar et al., 2020)
Log $P_{o:w}$	1.6	(Kovar et al., 2020)
pKa1, pKa2	8.1, 3.3	(Kovar et al., 2020)
Compound type	Diprotic base	
B/P	1.03	(Kovar et al., 2020)
f_u	0.951	(Kovar et al., 2020)
Distribution		

Model	Full PBPK	(Kovar et al., 2020)
Method	Rodger et al.	(Kovar et al., 2020)
Organ/tissue Kp		(Kovar et al., 2020)
Adipose	0.74	
Bone	1.27	
Brain	1.89	
Gut	2.90	
Heart	2.24	
Kidney	4.15	
Liver	3.96	
Lung	3.25	
Muscle	3.05	
Skin	1.1*	
Spleen	2.86	
Pancreas	2.46	
Kp scalar	1	
Elimination		
Organ/tissue: Liver		(Kovar et al., 2020)
Enzyme	CYP2A6	
k_{cat} (1/min) (smokers)	10.5	
K_m (μ M)	29.4	
$f_{u_{mic}}$	1	
V_{max} (μ mol/h)	979.8	
Enzyme	CYP2B6	
k_{cat} (1/min) (smokers)	16	
K_m (μ M)	820	
$f_{u_{mic}}$	1	
V_{max} (μ mol/h)	884.7	Eq. 55
Unspecified hepatic CL (1/min)	0.3	
Unspecified hepatic CL (L/min)	32.4	
CL_R in L/h	3.58	
Liver: CYP2A6		
A_{CYP2A6} (pmol/mg microsomal protein)	27	
A_{CYP2A6} (μ mol/liver tissue)	1.56	Eq. 58
Liver: CYP2B6		

A_{CYP2B6} (pmol/mg microsomal protein)	16	Eq. 58 (Barter et al., 2007) Table S5
A_{CYP2B6} (μ mol/liver tissue)	0.92	
Liver: PSF		
MMPGL (mg microsomal protein/g liver)	32	
Liver weight (g)	1800	Eq. 58
Lung: CYP2A6		
A_{CYP2A6} (pmol/mg microsomal protein) ¹	0.11	
A_{CYP2A6} (μ mol/liver tissue)	BB: 7E-6 bb: 4E-6 AL: 2E-4	
Lung: CYP2B6		Eq. 58
A_{CYP2B6} (pmol/mg microsomal protein) ¹	0.16	
A_{CYP2B6} (μ mol/lung tissue)	BB: 1E-5 bb: 5E-6 AL: 3E-4	
Lung: PSF		
MMPGLu (mg microsomal protein/g lung)	3.8	(Pacifici et al., 1988)

MW, molecular weight; Log $P_{o:w}$, n-octanol/water partition coefficient; pK_a , acid dissociation constant; B/P, blood/plasma ratio; f_u , fraction of unbound drug in the plasma; HSA, human serum albumin; K_p , tissue to plasma partition coefficient; k_{cat} , catalytic activity; V_{max} , maximum enzymatic reaction rate; K_m , Michaelis-Menten constant; $f_{u,mic}$, fraction of unbound drug in the *in vitro* microsomal incubation; CL_R , renal clearance; PSF, physiological scaling factor (yield of the subcellular fraction from whole organ (in mg subcellular fraction protein/g organ)); A_{DME} is the protein abundance of drug metabolizing enzymes (DME); CYP, cytochromes P450; MMPGL, mg microsomal protein per gram of human liver; MMPGLu, mg microsomal protein per gram of human lung.

*Huang and Isoherranen, 2020.

1. CYP2A6 and CYP2B6 protein abundance per subcellular fraction were calculated by multiplying the liver subcellular protein abundance by the ratio of lung (BB, bb, and AL) to liver tissue mRNA expression (Somers et al., 2007).

Table S8. Input and output for predicting the DE of morphine (administered via a nebulizer) in each region of the respiratory tract using the ICRP 66 deposition model.

Input for the ICRP 66 deposition model		
Parameters	Values	References
Drug parameters		
MMAD (μ m)	2.95	(Schuster et al., 1997)
GSD (dimensionless)	0	
Type	Monodisperse	Default (ICRP, 1995)
ρ (g/mL)	3	

X (dimensionless)	1.5	Default (ICRP, 1995)	
η_l (dimensionless)	1	Model predicted	
f_{hyg} (dimensionless)	3	Assumed	
DF_{scalar} (dimensionless)	1	Default	
Breathing parameters			
Breathing route	Mouth		
Activity type	Sitting		
Q (mL/s)	1208.33	(Dershwitz et al., 2000)	
V (mL)	500	(Dershwitz et al., 2000)	
U (m/s)	1	(Klumpp and Bertelli, 2017)	
Systems parameters			
FRC (mL)	3301	Adult male (ICRP, 1995)	
$V_{D,ET}$ (mL)	50	Adult male (ICRP, 1995)	
$V_{D,BB}$ (mL)	49	Adult male (ICRP, 1995)	
$V_{D,bb}$ (mL)	47	Adult male (ICRP, 1995)	
$V_{D,total}$ (mL)	146	Adult male (ICRP, 1995)	
SF_{BB} (dimensionless)	1	Adult male (ICRP, 1995)	
SF_{bb} (dimensionless)	1	Adult male (ICRP, 1995)	
SF_{AL} (dimensionless)	1	Adult male (ICRP, 1995)	
Output of the ICRP 66 deposition model			
Region	DE	DE with f_{hyg}	<i>In vivo</i> DE
ET2	19.2	33.0	NA
BB	16.0	19.5	NA
bb	7.1	8.1	NA
TB (BB+bb)	23.2	27.6	NA
AL	10.4	12.3	NA
Total	52.8	72.9	NA
Exhaled	47.2	27.1	NA
TB (central)/AL (peripheral)	2.22	2.24	NA

MMAD, mass median aerodynamic diameter; GSD, geometric standard deviation of aerodynamic diameter; Q, volumetric or inhalation flow rate; V, tidal or inhalation volume; DE, deposition efficiency (%); ET2, extrathoracic (oral passage); BB, bronchial; bb, bronchiolar; TB, tracheobronchial; AL, alveolar; f_{hyg} , hygroscopic growth factor; DF_{scalar} , empirical scaling factor to scale regional deposition fraction; ρ , drug density; χ , shape factor; η_i , inhalability.

Table S9. Input and output for predicting the DE of nicotine (administered via cigarette smoking) in each region of the respiratory tract using the ICRP 66 deposition model.

Input for the ICRP 66 deposition model				
Parameters	Values	References		
Drug parameters				
MMAD (μm)	0.4	(Schroeter et al., 2001)		
GSD (dimensionless)	0			
Type	Monodisperse			
ρ (g/mL)	3	Default (ICRP, 1995)		
X (dimensionless)	1.5	Default (ICRP, 1995)		
η _l (dimensionless)	1	Model predicted		
f _{hyg} (dimensionless)	1.7	(Schroeter et al., 2001)		
DF _{scalar} (dimensionless)	1.5	Estimated to recover <i>in vivo</i> deposition		
Breathing parameters				
Breathing route	Mouth			
Activity type	Sitting			
Q (mL/s)	17.5	Calculated using puff volume (35 mL) and puff time (2 s) (Kane et al., 2010)		
V (mL)	500	(Kane et al., 2010)		
U (m/s)	1	(Klumpp and Bertelli, 2017)		
Systems parameters				
FRC (mL)	3301	Adult male (ICRP, 1995)		
V _{D,ET} (mL)	50	Adult male (ICRP, 1995)		
V _{D,BB} (mL)	49	Adult male (ICRP, 1995)		
V _{D,bb} (mL)	47	Adult male (ICRP, 1995)		
V _{D,total} (mL)	146	Adult male (ICRP, 1995)		
SF _{BB} (dimensionless)	1	Adult male (ICRP, 1995)		
SF _{bb} (dimensionless)	1	Adult male (ICRP, 1995)		
SF _{AL} (dimensionless)	1	Adult male (ICRP, 1995)		
Output of the ICRP 66 deposition model				
Region	DE	DE with f _{hyg}	DE with f _{hyg} and DF _{scalar}	<i>In vivo</i> DE
ET2	1.0	0.7	1.1	
BB	2.0	1.3	2.0	
bb	31.3	41.1	61.7	
TB (BB + bb)	33.3	42.4	63.7	42-63*
AL	21.4	20.8	31.2	26-35*

Total	55.7	64	96.0	86-97 [#]
Exhaled	44.3	36	4.0	
TB (central)/AL (peripheral)	1.55	2.04	2.04	

MMAD, mass median aerodynamic diameter; GSD, geometric standard deviation of aerodynamic diameter; Q, volumetric or inhalation flow rate; V_T , tidal or inhalation volume; ET2, extrathoracic (oral passage); BB, bronchial; bb, bronchiolar; TB, tracheobronchial; AL, alveolar; f_{hyg} , hygroscopic growth factor; DF_{scalar} , empirical scaling factor to scale regional deposition fraction; ρ , drug density; χ , shape factor; η_i , inhalability; DE, deposition efficiency in percent.

*(Broday and Robinson, 2003), #(Hinds et al., 1983)

Table S10. Summary of input parameters for morphine and nicotine OI model.

Parameter	Morphine	Nicotine	Equations
$K_{p_{int-pls}}$	0.74	0.93	Eq. 38
$P_{app, calu-3}$ (cm/s)	4.54E-06	8.62E-06	Eq. 42
P_{scalar}	2.4	-	
Thickness factor			Eq. 41
ET2	1.10	1.10	
BB	1.00	1.00	
bb	3.67	3.67	
AL	152.35	152.35	
$P_{app, n}$ (cm/s)			Eq. 40
ET2	4.99E-06	9.48E-06	
BB	4.54E-06	8.62E-06	
bb	1.66E-05	3.16E-05	
AL	6.92E-04	1.31E-03	
P_{mem} or PS (L/h)			Eq. 39
ET2	1.94E-02	1.54E-02	
BB	1.14E-02	9.00E-03	
Bb	3.46E-01	2.73E-01	
AL	8.81E+03	6.97E+03	
Regions: ET2, BB, bb and AL			Eqs. 28-33
f_{uiF}	0.04	0.97	
f_{uiE}	0.06	0.96	
f_{uiS}	0.21	0.15	
f_{uiB}	0.23	0.17	
Regions: ET2, BB, bb and AL			Eqs. 34-37

f _{uF}	1	1	
f _{uE}	0.31	0.29	
f _{uS}	0.84	1	
f _{uB}	0.57	0.92	
Regions: ET2, BB, bb and AL CL _{inf} ,F-E (L/h) CL _{eff} ,E-F (L/h) CL _{inf} ,S-E (L/h) CL _{eff} ,E-S (L/h)	NA NA NA NA	NA NA NA NA	
Regions: ET2, BB, bb and AL CL _{int} (L/h)	NA	NA	
Regions: ET2, BB, bb and AL k _{deg} (1/h)	NA	NA	
Regions: ET2, BB, bb and AL k _{on} (L/mg/h) k _{off} (1/h)	NA NA	NA NA	

Table S11. Comparison of simulated and observed PK parameters of morphine after IV infusion (IV Inf) or oral inhalation (OI; nebulizer)

Study ID	Dosing regimen	PK parameters	Simulated	Observed	Ratio
Dershwitz et al_2000	IV Inf Dose: 8.8 mg Duration: 0.16 h	C _{max}	258.0	261.1	0.99
		AUC _{last}	66.8	66.05	0.97
Dershwitz et al_2000 (without f _{hyg})	OI (dose: 2.2 mg, no. of dose: 8; interval: 1 min)	C _{max}	76.5	120.3	0.64
		AUC _{last}	37.8	71.8	0.53
Dershwitz et al_2000 (with f _{hyg})	OI (dose: 2.2 mg, no. of dose: 8; interval: 1 min)	C _{max}	91.8	120.3	0.76
		AUC _{last}	46.5	71.8	0.65
Dershwitz et al_2000 (with f _{hyg} and P _{scalar})	OI (dose: 2.2 mg, no. of dose: 8; interval: 1 min)	C _{max}	139.4	120.3	1.16
		AUC _{last}	65.3	71.8	0.91

f_{hyg}, hygroscopic growth factor; P_{scalar}, permeability scalar, used to scale the epithelial apical permeability; C_{max}, maximum plasma concentration; AUC_{last}, area under the plasma concentration-time curve from 0 to the last measured time point.

Table S12. Comparison of the simulated and observed PK parameters of nicotine after IV infusion.

Study ID	Dosing regimen	PK parameters	Simulated	Observed	Ratio
Gourlay and Benowitz_1997	IV Inf (4.38 mg)	C _{max}	28.1	28.65	0.98
		AUC _{0-last}	17.5	19.44	0.90
Benowitz and Jacob_1994	IV Inf (60 µg/kg)	C _{max}	27.1	24.06	1.13
		AUC _{0-last}	50.6	51.24	0.99

Table S13. Comparison of the simulated and observed PK parameters of nicotine after oral inhalation (cigarette smoking) when f_{hyg} and DF_{scalar} were incorporated.

Study ID	Dosing regimen*	PK parameters	Simulated	Observed	Ratio
Gourlay and Benowitz 1997	OI (Dose: 0.22 mg; No. of puff: 10; Puff interval: 1 min)	C _{max}	19.9	19.18	1.04
		AUC _{0-last}	11.1	10.36	1.07
Fearson et al. 2017	OI (Dose: 0.13 mg; No. of puff: 10; Puff interval: 0.0083 h)	C _{max}	12.2	11.95	1.02
		AUC _{0-last}	2.4	2.12	1.14
Fearson et al. 2017	OI (Dose: 0.07 mg; No. of puff: 10; Puff interval: 0.0083 h)	C _{max}	6.6	6.29	1.04
		AUC _{0-last}	3.6	3.59	1.01
St. Helen et al. 2019	OI (Dose: 0.24 mg; No. of puff: 10; Puff interval: 0.0083 h)	C _{max}	22.5	20.53	1.09
		AUC _{0-last}	25.7	23.05	1.11

*doses adopted from Kovar et al., 2020.

Supplemental Figures

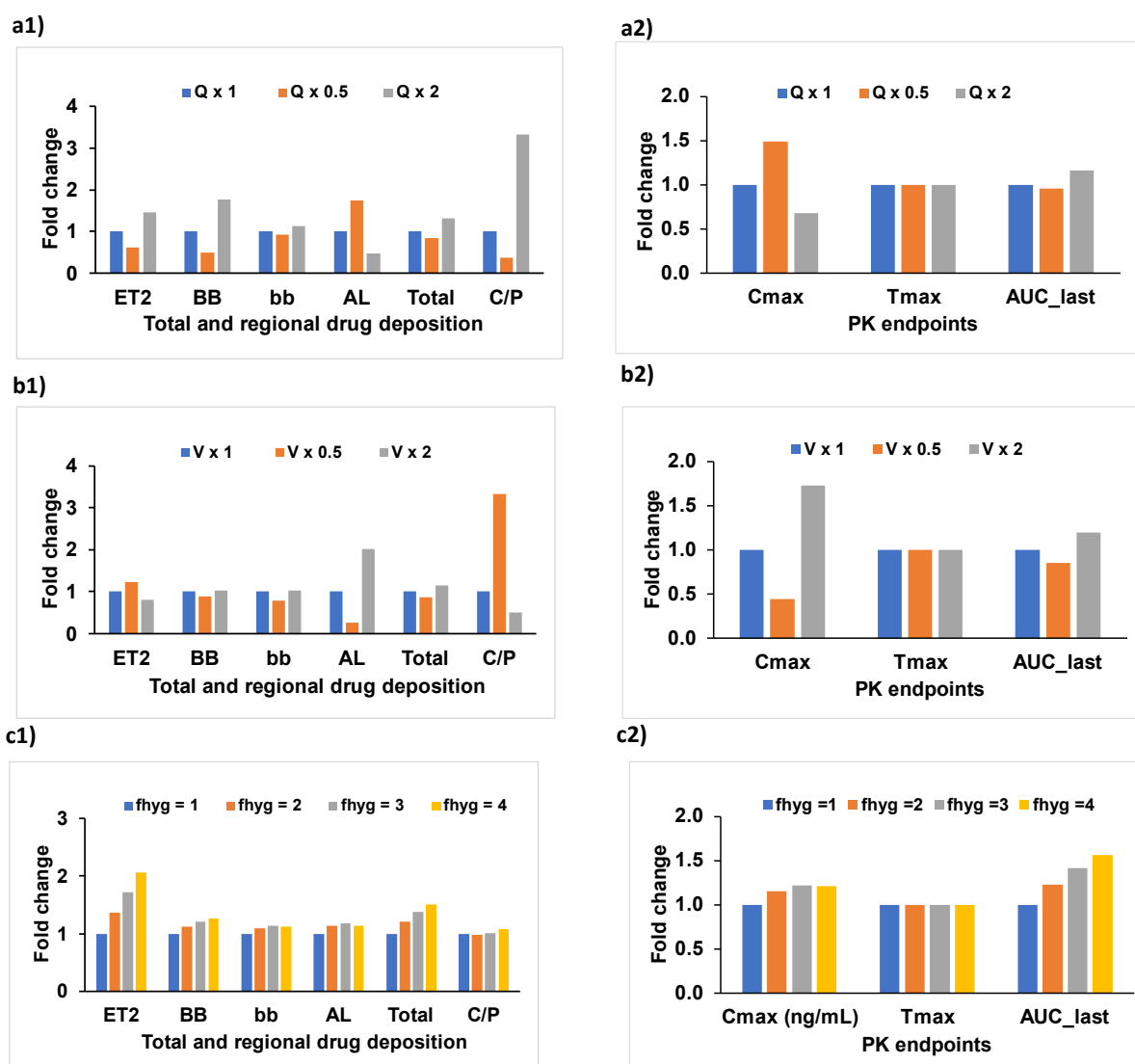


Fig. S1. Sensitivity analyses to demonstrate the impact of change in inhalation flow (a1 and a2), inhalation volume (V; b1 and b2), and hygroscopic growth factor (f_{hyg} ; c1 and c2)) on total and regional respiratory tract deposition, as well as pharmacokinetic (PK) endpoints of drug X. ET2, extrathoracic (oral passage); BB, bronchial; bb, bronchiolar; AL, alveolar; C, central region (BB+bb); P, peripheral region (AL).

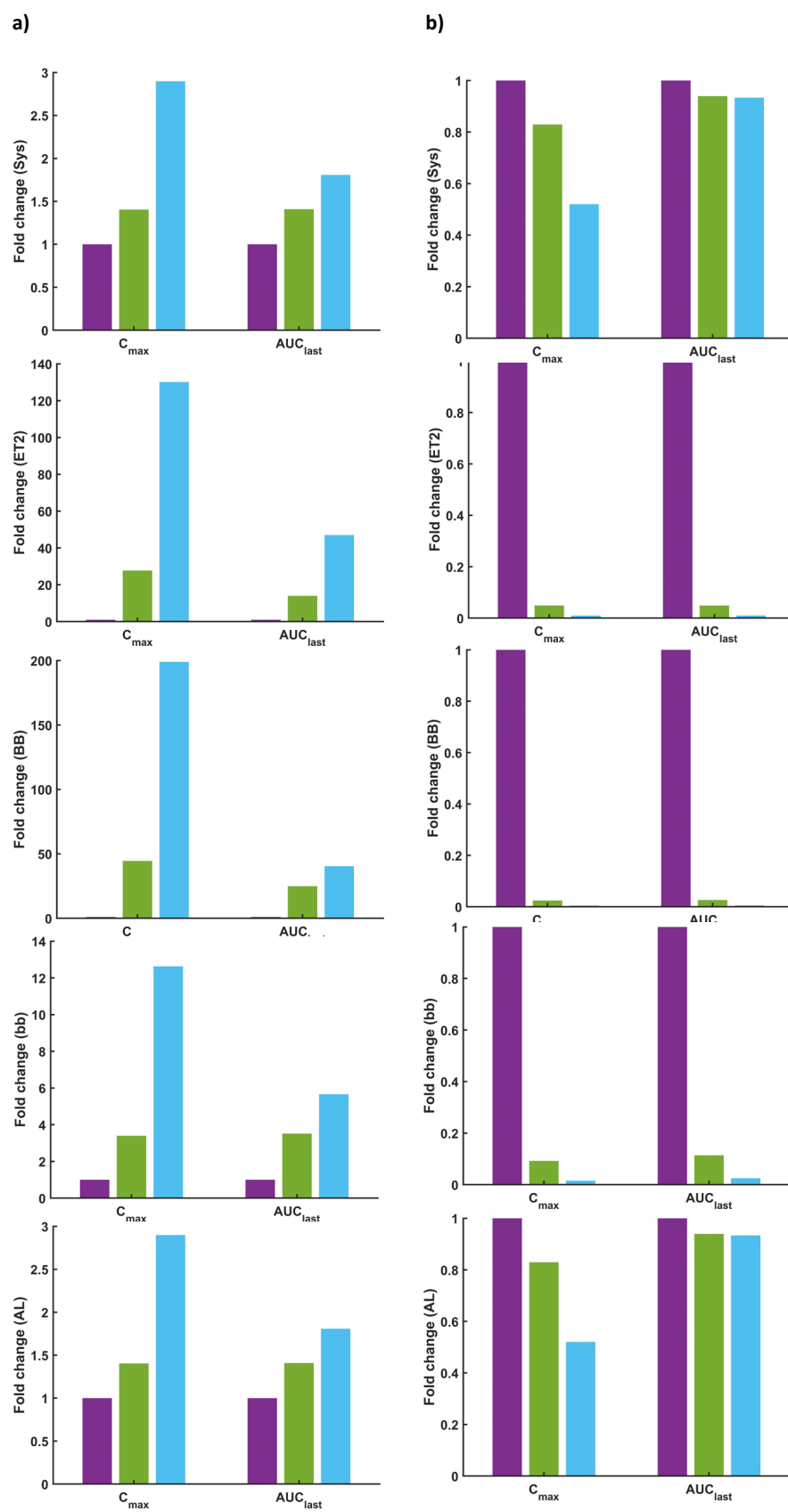


Fig. S2. Sensitivity analyses to demonstrate the impact of epithelial membrane transport on systemic and local epithelial concentrations of drug Y in various regions of the respiratory

tract (ET2, BB, bb and AL) in the presence of a) apical influx transport (clearance: 0 L/h, purple color; 0.0001 L/h, green color; 0.0005 L/h, sky blue color); or b) apical efflux transport (clearance: 0 L/h, purple color; 50 L/h, green color; 250 L/h, sky blue color). In all the cases, low apparent passive permeability (4.54×10^{-8} cm/s) between ELF and epithelial was unchanged. Increased influx or efflux apical epithelial membrane transport results in either increased (influx) or reduced (efflux) drug Y epithelial concentrations in all the regions of the respiratory tract except for the AL region (because of the lower drug's AL deposition in the ELF compartment and large AL surface area, resulting in high passive drug permeability).

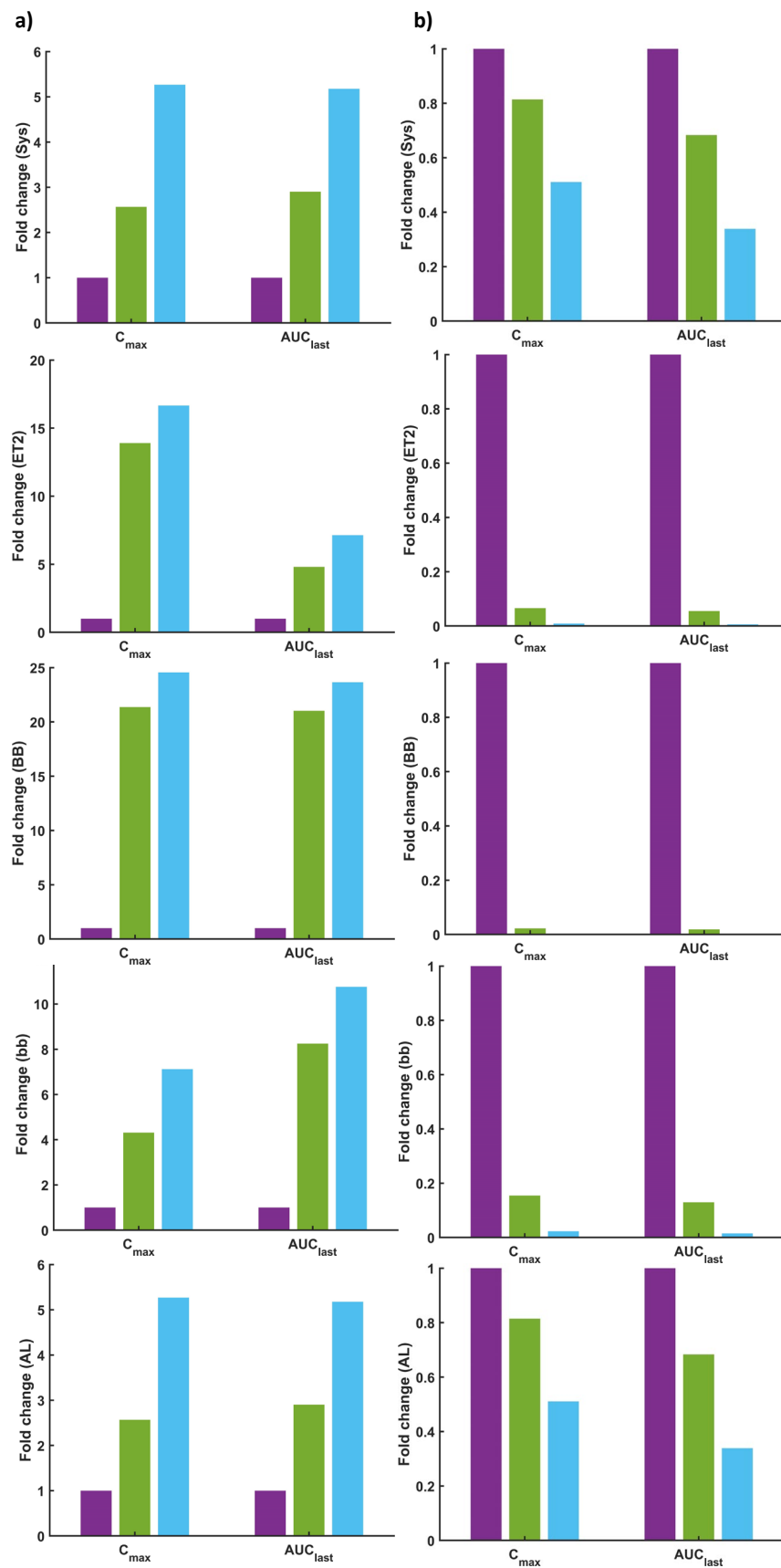


Fig. S3. Sensitivity analyses to demonstrate the impact of apical subepithelial membrane (or basal epithelial membrane) transport on systemic and local subepithelial concentrations of

drug Y in various respiratory tract compartments (ET2, BB, bb and AL) in the presence of a) influx transport (clearance: 0 L/h, purple color; 50 L/h, green color; 250 L/h, sky blue color); or b) efflux transport (clearance: 0 L/h, purple color; 10 L/h, green color; 50 L/h, sky blue color). In all the cases, low apparent passive permeability (4.54×10^{-8} cm/s) between ELF and epithelial as well as epithelial and subepithelial was unchanged. Increased influx or efflux subepithelial membrane transporter activity results in increased (influx) or reduced (efflux) drug Y epithelial concentrations in all the regions of the respiratory tract.

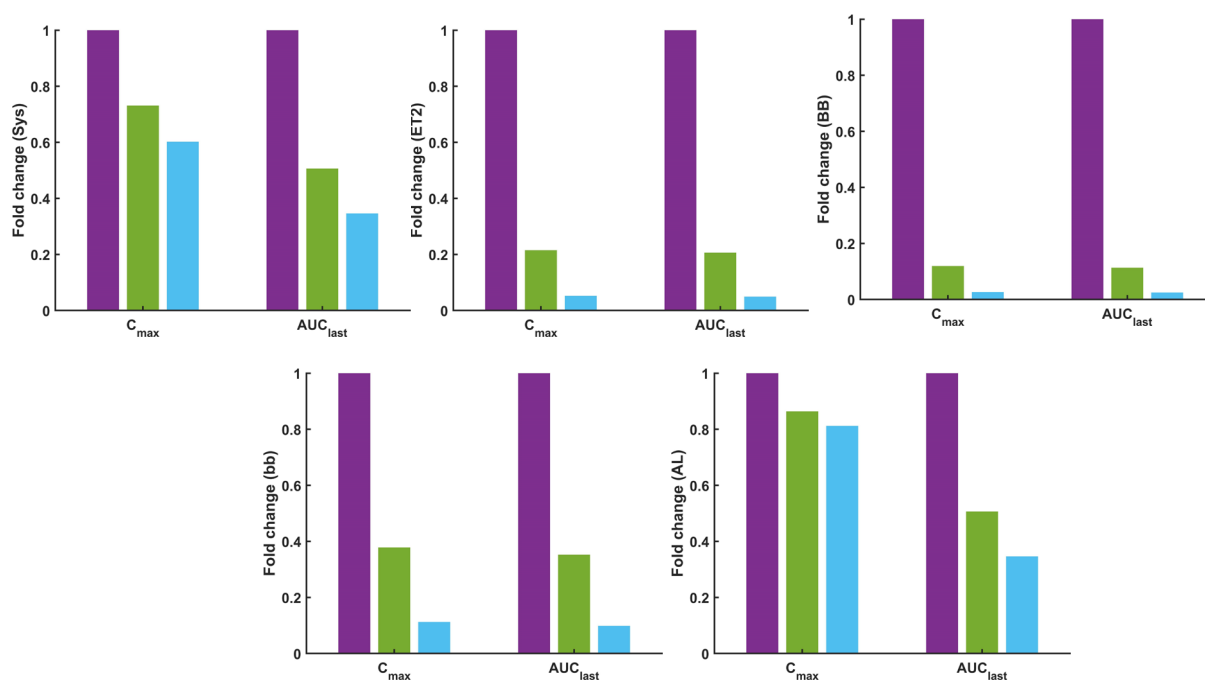


Fig. S4. Sensitivity analyses to demonstrate the impact of epithelial metabolism on systemic and local epithelial concentrations of drug Y in various lung compartments (ET2, BB, bb and AL) in the presence of metabolism (clearance: 0 L/h, purple color; 10 L/h, green color; 50 L/h, sky blue color). Increased drug metabolic activity in the epithelial region, decreased systemic and regional exposure of drug Y.

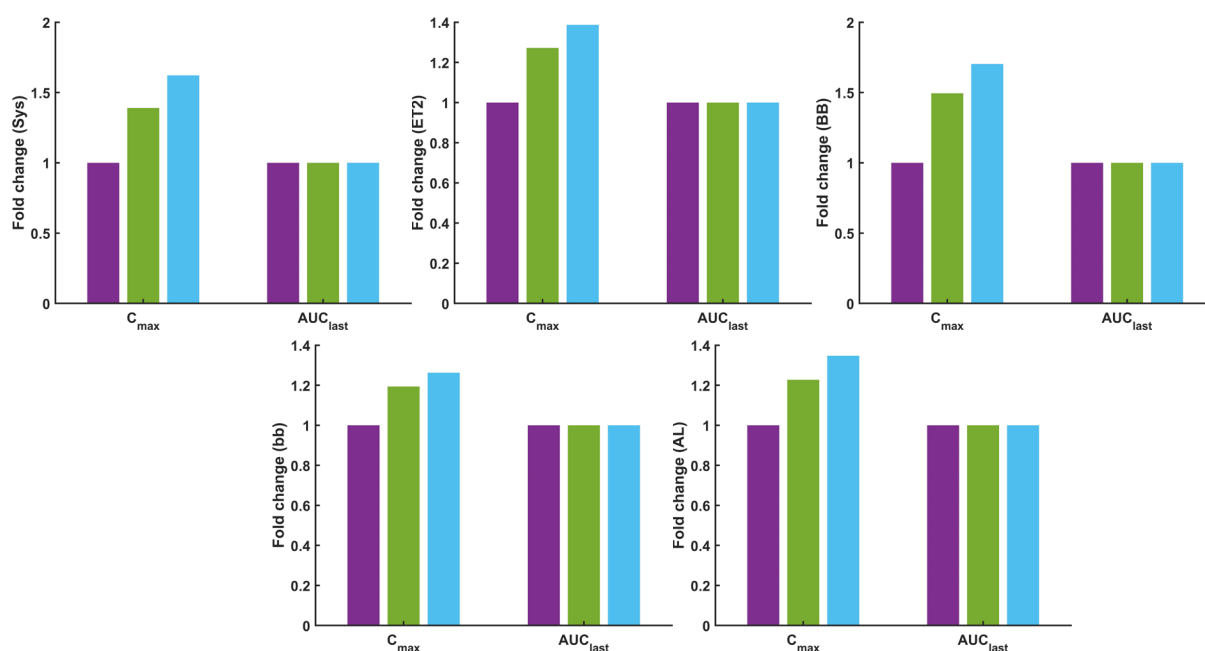


Fig. S5. Sensitivity analyses to demonstrate the impact of tissue retention on systemic and local epithelial concentrations of drug Y in various respiratory tract compartments (ET2, BB, bb and AL) in the presence of tissue retention (dissociation rate constant: 10 1/h, purple color; 50 1/h, green color; 250 1/h, sky blue color; in all these cases, the association rate constant and fatty acid concentrations were fixed to 50 L/mg/h and 10.0 mg/L). Increased dissociation rate constant in the epithelial region, increased systemic and regional C_{max} but did not change exposure to drug Y (AUC_{last}).

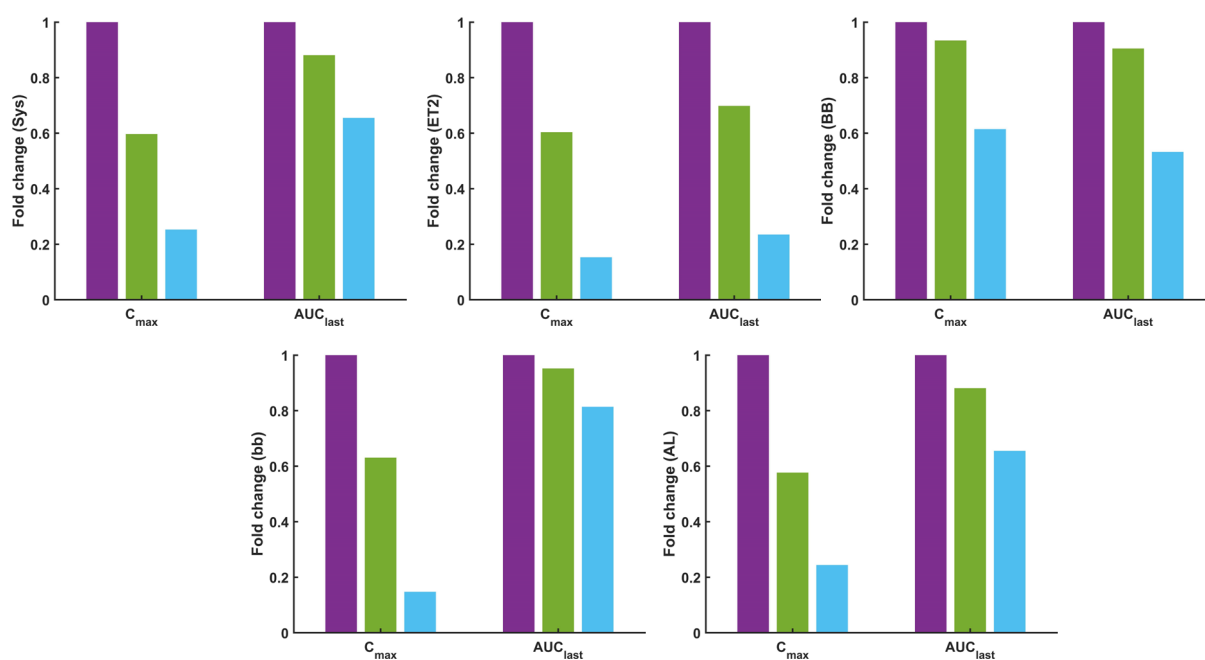


Fig. S6. Sensitivity analyses to demonstrate the impact of dissolution rate (z-factor) on systemic and local epithelial concentrations of drug X in various respiratory tract compartments (ET2, BB, bb and AL) in the presence of dissolution rate (z-factor 0.01 L/mg/h, purple color; 0.001 L/mg/h, green color; 0.0001 L/mg/h, sky blue color). Decreased in the dissolution rate of drug X resulted in a decrease in both local and systemic C_{max} as well as AUC_{last} due to slow drug release in the airway fluid.

References:

- Barter ZE, Chowdry JE, Harlow JR, Snawder JE, Lipscomb JC, Rostami-Hodjegan A (2008) Covariation of human microsomal protein per gram of liver with age: absence of influence of operator and sample storage may justify interlaboratory data pooling. *Drug Metabolism and Disposition* **36**:2405-9.
- Brillault J, De Castro WV, and Couet W (2010) Relative contributions of active mediated transport and passive diffusion of fluoroquinolones with various lipophilicities in a Calu-3 lung epithelial cell model. *Antimicrobial Agents and Chemotherapy* **54**:543-545.
- Broday DM and Robinson R (2003) Application of cloud dynamics to dosimetry of cigarette smoke particles in the lungs. *Aerosol Science & Technology* **37**:510-527.
- Burton RF (2001) Differences in pH between interstitial fluid and arterial blood in water-breathing and air-breathing vertebrates. *Physiological and Biochemical Zoology* **74**:607-615.
- Chen B, Namenyi J, Yeh H, Mauderly J, and Cuddihy R (1990) Physical characterization of cigarette smoke aerosol generated from a Walton smoke machine. *Aerosol Science and Technology* **12**:364-375.
- Dershwitz M, Walsh JL, Morishige RJ, Connors PM, Rubsamen RM, Shafer SL, and Rosow CE (2000) Pharmacokinetics and pharmacodynamics of inhaled versus intravenous morphine in healthy volunteers. *The Journal of the American Society of Anesthesiologists* **93**:619-628.
- Emoto C, Fukuda T, Johnson T, Neuhoﬀ S, Sadhasivam S, and Vinks A (2017) Characterization of contributing factors to variability in morphine clearance through PBPK modeling implemented with OCT1 transporter. *CPT: pharmacometrics & Systems Pharmacology* **6**:110-119.
- Gaohua L, Wedagedera J, Small B, Almond L, Romero K, Hermann D, Hanna D, Jamei M, and Gardner I (2015) Development of a multicompartment permeability-limited lung pbpk model and its application in predicting pulmonary pharmacokinetics of antituberculosis drugs. *CPT: Pharmacometrics & Systems Pharmacology* **4**:605-613.
- Hinds W, First M, Huber G, and Shea J (1983) A method for measuring respiratory deposition of cigarette smoke during smoking. *American Industrial Hygiene Association Journal* **44**:113-118.
- Hintz RJ and Johnson KC (1989) The effect of particle size distribution on dissolution rate and oral absorption. *International Journal of Pharmaceutics* **51**:9-17.
- ICRP (1995) ICRP publication 66: human respiratory tract model for radiological protection. Elsevier Health Sciences.
- Kane DB, Asgharian B, Price OT, Rostami A, and Oldham MJ (2010) Effect of smoking parameters on the particle size distribution and predicted airway deposition of mainstream cigarette smoke. *Inhalation Toxicology* **22**:199-209.
- Klumpp J and Bertelli L (2017) KDEP: a resource for calculating particle deposition in the respiratory tract. *Health Physics* **113**:110-121.
- Kovar L, Selzer D, Britz H, Benowitz N, St. Helen G, Kohl Y, Bals R, and Lehr T (2020) Comprehensive parent-metabolite PBPK/PD modeling insights into nicotine replacement therapy strategies. *Clinical Pharmacokinetics* **59**:1119-1134.
- Ladumor MK, Thakur A, Sharma S, Rachapally A, Mishra S, Bobe P, Rao VK, Pammi P, Kangne H, Levi D, Balhara A, Ghandikota S, Joshi A, Nautiyal V, Prasad B, and Singh S (2019) A repository of protein abundance data of drug metabolizing enzymes and transporters for applications in physiologically based pharmacokinetic (PBPK) modelling and simulation. *Scientific Reports* **9**:9709.
- Ohtsuki S, Schaefer O, Kawakami H, Inoue T, Liehner S, Saito A, Ishiguro N, Kishimoto W, Ludwig-Schwellinger E, Ebner T, Terasaki T (2012) Simultaneous absolute protein quantification of transporters, cytochromes P450, and UDP-glucuronosyltransferases as a novel approach for the characterization of individual human liver: comparison with mRNA levels and activities. *Drug metabolism and Disposition* **40**:83-92.

- Pacifici GM, Franchi M, Bencini C, Repetti F, Di Lascio N, Muraro GB (1988) Tissue distribution of drug-metabolizing enzymes in humans. *Xenobiotica* **18**:849-56.
- Patton JS and Byron PR (2007) Inhaling medicines: delivering drugs to the body through the lungs. *Nature Reviews Drug Discovery* **6**:67-74.
- Po HN and Senozan N (2001) The Henderson-Hasselbalch equation: its history and limitations. *Journal of Chemical Education* **78**:1499.
- Prasad B, Evers R, Gupta A, Hop CE, Salphati L, Shukla S, Ambudkar SV, Unadkat JD (2014) Interindividual variability in hepatic organic anion-transporting polypeptides and P-glycoprotein (ABCB1) protein expression: quantification by liquid chromatography tandem mass spectroscopy and influence of genotype, age, and sex. *Drug Metabolism and Disposition* **42**:78-88.
- Sakamoto A, Matsumaru T, Yamamura N, Uchida Y, Tachikawa M, Ohtsuki S, and Terasaki T (2013) Quantitative expression of human drug transporter proteins in lung tissues: analysis of regional, gender, and interindividual differences by liquid chromatography-tandem mass spectrometry. *Journal of Pharmaceutical Sciences* **102**:3395-3406.
- Schmitt W (2008). General approach for the calculation of tissue to plasma partition coefficients. *Toxicology In Vitro* **22**:457-67.
- Schroeter JD, Musante CJ, Hwang D, Burton R, Guilmette R, and Martonen TB (2001) Hygroscopic growth and deposition of inhaled secondary cigarette smoke in human nasal pathways. *Aerosol Science & Technology* **34**:137-143.
- Schuster J, Rubsam R, Lloyd P, and Lloyd J (1997) The AERx™ aerosol delivery system. *Pharmaceutical Research* **14**:354-357.
- Shah DK, Betts AM (2012) Towards a platform PBPK model to characterize the plasma and tissue disposition of monoclonal antibodies in preclinical species and human. *Journal of Pharmacokinetics and Pharmacodynamics* **39**:67-86.
- Somers GI, Lindsay N, Lowdon BM, Jones AE, Freathy C, Ho S, Woodrooffe AJ, Bayliss MK, Manchee GR (2007) A comparison of the expression and metabolizing activities of phase I and II enzymes in freshly isolated human lung parenchymal cells and cryopreserved human hepatocytes. *Drug metabolism and disposition*. **35**:1797-805.
- Valentin J (2002) Basic anatomical and physiological data for use in radiological protection: reference values: ICRP Publication 89. *Annals of the ICRP* **32**:1-277.
- Wang L, Prasad B, Salphati L, Chu X, Gupta A, Hop CE, Evers R, Unadkat JD (2015) Interspecies variability in expression of hepatobiliary transporters across human, dog, monkey, and rat as determined by quantitative proteomics. *Drug Metabolism and Disposition* **43**:367-74.